NeuroImage 49 (2010) 2862–2870

Contents lists available at ScienceDirect

NeuroImage

journal homepage: www.elsevier.com/locate/ynimg

Spatial and temporal EEG dynamics of motion sickness

Yu-Chieh Chen [a,b], Jeng-Ren Duann [a,d], Shang-Wen Chuang [a,c], Chun-Ling Lin [a,b], Li-Wei Ko [a,b], Tzyy-Ping Jung [a,d], Chin-Teng Lin [a,b,*]

[a] Brain Research Center, University System of Taiwan, Hsinchu, Taiwan
[b] Department of Electrical and Control Engineering, National Chiao-Tung University, Hsinchu, Taiwan
[c] Department of Computer Science, National Chiao-Tung University, Hsinchu, Taiwan
[d] Institute for Neural Computation, University of California, San Diego, CA, USA

ARTICLE INFO

Article history:
Received 17 August 2009
Revised 2 October 2009
Accepted 2 October 2009
Available online 13 October 2009

Keywords:
EEG
Independent component analysis (ICA)
Motion sickness
Time frequency
Vestibular system
Brain dynamics

ABSTRACT

This study investigates motion-sickness-related brain responses using a VR-based driving simulator on a motion platform with six degrees of freedom, which provides both visual and vestibular stimulations to induce motion sickness in a manner that is close to that in daily life. Subjects' brain dynamics associated with motion sickness were measured using a 32-channel EEG system. Their degree of motion sickness was simultaneously and continuously reported using an onsite joystick, providing non-stop behavioral references to the recorded EEG changes. The acquired EEG signals were parsed by independent component analysis (ICA) into maximally independent processes. The decomposition enables the brain dynamics that are induced by the motion of the platform and motion sickness to be disassociated. Five MS-related brain processes with equivalent dipoles located in the left motor, the parietal, the right motor, the occipital and the occipital midline areas were consistently identified across all subjects. The parietal and motor components exhibited significant alpha power suppression in response to vestibular stimuli, while the occipital components exhibited MS-related power augmentation in mainly theta and delta bands; the occipital midline components exhibited a broadband power increase. Further, time series cross-correlation analysis was employed to evaluate relationships between the spectral changes associated with different brain processes and the degree of motion sickness. According to our results, it is suggested both visual and vestibular stimulations should be used to induce motion sickness in brain dynamic studies.

Introduction

Motion sickness (MS) is a common experience of numerous people and has motivated extensive physiological, neurophysiological and psychophysiological research. The focus of early motion-sickness studies was on the physiological changes related to motion sickness. For instance, the electrogastrography (EGG) signals (Hu et al., 1991; Cheung and Vaitkus, 1998) have been employed to detect symptoms of motion sickness, such as vomiting, and galvanic skin responses (GSR) have been used to detect sweating. Holmes and Griffin (2001) observed increased heart rate variability (HRV) during nausea, indicating the modulation of the automatic nervous system (ANS) in motion sickness. Rapid advances in neuroimaging technology have enabled the neural correlates of motion sickness to be examined. Electroencephalography (EEG) is one of the best methods for monitoring the brain dynamics induced by motion sickness because of its high temporal resolution and portability. Wu (1992) showed that theta power increases in the frontal and central areas when subjects were placed and moved in a parallel swing device. Wood et al. (1991, 1994) also found increased EEG theta wave in the frontal areas during motion sickness induced by a rotating drum. Chelen et al. (1993) adopted cross-coupled angular stimulation to induce motion sickness and found increased delta- and theta-band power during sickness but no significant change in alpha power. Hu et al. (1999) investigated MS triggered by the viewing of an optokinetic rotating drum and found a higher net percentage increase in EEG power in the 0.5- to 4-Hz band at electrode sites C3 and C4 than in the baseline spectra. Kim et al. (2005) found increases in both delta and beta power in the frontal and temporal areas in an object-finding VR experiment. Min et al. (2004) also found increases in delta power in a car-driving VR experiment. However, they also found that theta power declined as the degree of motion sickness increased.

Motion-sickness-induced EEG power changes are not consistent among all of the cited studies. One reason may be the wide range of paradigms used to induce motion sickness. Most of the above-mentioned experiments involved a single modality using either visual (Hu et al., 1999; Kim et al., 2005; Lo and So, 2001; Min et al., 2004) or vestibular inputs (Wood et al., 1991, 1994; Wu, 1992; Chelen et al., 1993). This single-modality scheme may be unrealistic and suboptimal

* Corresponding author. Brain Research Center, National Chiao-Tung University (NCTU), 1001 Ta-Hsueh Road, Hsinchu, Taiwan 300, ROC. Fax: +886 3 572 6272.
E-mail address: ctlin@mail.nctu.edu.tw (C.-T. Lin).

1053-8119/$ – see front matter © 2009 Elsevier Inc. All rights reserved.
doi:10.1016/j.neuroimage.2009.10.005

for reliably inducing motion sickness in subjects and, leading to inconsistent results concerning changes in EEG power.

Another important factor in motion-sickness experiments has been the degree of sickness of the participants. Many scholars have adopted a motion-sickness questionnaire by Kennedy et al. (1993) to measure susceptibility of subjects to MS. It is a standard rating system for comparing MS states among subjects. However, it demands interrupting the experiments and asking the subjects to answer few questions. This approach may not be practical for a continuous performance task, in which subjects must perform the task continuously. For example, in a long-term driving experiment in which the subject's cognitive states are monitored, interrupting the experiment for the questionnaire may arouse the subjects. Moreover, such intervention may influence human physiology which makes correlating the measured physiological signals with the motion-sickness level very difficult or even impossible. Therefore, an easy-to-operate online rating mechanism is sought to record continuously the level of motion sickness in subjects.

This study demonstrates a VR-based motion-sickness platform that comprises a 32-channel EEG system and a joystick with a continuous scale, which subjects can continuously report their level of motion sickness during experiments. All measurements, including of the level of motion sickness and of the motion of the platform, were synchronized with the EEG recordings. The VR-based platform simultaneously provides both visual and vestibular stimuli to generate a most realistic experimental environment for studying motion sickness. The recorded EEG signals are analyzed using independent component analysis (ICA), time-frequency analysis and time-series cross-correlation to investigate MS-related brain dynamics in a continuous driving task.

Materials and methods

Unlike previous investigations, this study provides both visual and vestibular stimuli to the subjects in a realistic environment that comprises a 360° projection of VR scene and motion platform with six degrees of freedom (DOF) to induce motion sickness. It is expected to induce motion sickness in a manner consistent with real-life experience. During the experiments, the subjects were asked to sit as passengers inside a model car that was mounted on the motion platform, with their hands on a joystick that was used to report continuously their sickness level.

Experimental protocol

An auto-driving VR scene in a tunnel was programmed to eliminate any possible visual distraction and shorten the depth of the visual field such that motion sickness could be easily induced. A three-section experimental protocol (Fig. 2A) was designed to induce motion sickness. First, the baseline section involved 10 min of driving on a straight road to record the subjects' baseline EEG. Then, a winding road was presented to the subjects for 40 min to induce motion sickness. Finally, a recovery section that involved cruising on a straight road was presented for 15 min to help the subjects to recover from the sickness. The level of sickness was continuously reported by the subjects, using a joystick with a continuous scale on its side. The experimental setting successfully induced motion sickness in more than 80% of the subjects herein this investigation.

Participants

Twenty-four healthy, right-handed volunteers (15 males and nine females, aged 21 to 24 years old, with an average age of 22.1 years old) with no history of gastrointestinal, cardiovascular or vestibular disorders or of drug or alcohol abuse, taking no medication and with normal or corrected-to-normal vision participated in this experiment. Among the 24 participants, four (16.67%) experienced no motion sickness at all (subjects 1, 8, 12 and 16) and one became so sick (subject 14, 4.17%) that he or she was excluded from further data analysis. The EEG data recorded from the remaining 19 subjects were used to examine the brain dynamics during MS.

Signal acquisition

Thirty two-channel EEG signals were acquired at a sampling rate of 500 Hz using a NuAmps (BioLink Ltd., Australia). The electrode locations were based on a standard thirty two-channel system provided in a freely downloadable Matlab toolbox, EEGLAB (http://sccn.ucsd.edu/eeglab). The acquired EEG signals were first inspected to remove bad EEG channels and then down-sampled to 250 Hz. A high-pass filter with a cut-off frequency at 1 Hz with a transition band of 0.2 Hz was used to remove baseline-drifting artifacts. Then, a low-pass filter with a cut-off frequency of 50 Hz and a transition band of 7 Hz was applied to the signal to remove muscular artifacts and line noise. During each experiment, the level of sickness was continuously reported by each subject using a joystick with a continuous scale, which was synchronized to the EEG signals. The subjects were told to push the joystick to a higher level if they felt more sick comparing to the last condition. The sickness level ranged from zero to five. This continuous sickness level was reported in real time without interrupting the experiment rather than the traditional motion-sickness questionnaire (MSQ). A moving 100-s window was applied to smooth the continuous subjective sickness ratings using steps of 1 s. Fig. 3A displays an example of a smoothed single-subject sickness level. Notably, the traditional MSQ was applied after each experiment to provide overall motion-sickness rating information.

ICA and IC clusters

The filtered EEG signals were first decomposed into independent brain sources by independent component analysis (ICA) (Bell and Sejnowski, 1995; Makeig et al., 1997) using EEGLAB (Delorme and Makeig, 2004). The ICA algorithm can separate N source components from N channels of EEG signals. The summation of the EEG signals at the sensors is assumed to be linear and instantaneous, i.e., the propagation delays are negligible. We also assume that the time courses of muscle activity, eye and cardiac signals are not time locked to the EEG activities reflecting synaptic activity of cortical neurons. Therefore, the time courses of the sources are assumed to be statistically independent. The multi-channel EEG recordings are considered as mixtures of underlying brain sources and artificial signals. The source signals contribute to the scalp EEG signals through a fixed spatial filter. Such a spatial filter can be reflected by the rows of inverse of unmixing matrix, W in $u = Wx$, where u is the source matrix and x is the scalp-recorded EEG. The spatial filters can be plotted as the scalp topography of independent component. The scalp topography of each independent component (IC) can be further analyzed using DIPFIT2 routines (Oostendorp and Oostenveld, 2002), a plug-in in EEGLAB, to find the 3D location of an equivalent dipole or dipoles based on a four-shell spherical head model. Then, components with similar scalp topographies, dipole locations and power spectra from many subjects were further grouped into component clusters to examine the consistency of brain areas involved in the task. Ten component clusters recruited more than 10 components from multiple subjects with similar topographic maps. Among these robust component clusters, we further correlated the component power spectra with subjects' continuous motion-sickness rating. Average correlation coefficient was computed for each of the robust component clusters. Then, the five most motion sickness level-related clusters were selected for further analysis.

It has been shown that ICA is capable of reliably separating the eye activities, such as eye blinking, lateral eye movements (LEM) (Jung et

al., 2000). Here, we can use the robust eye-activity component(s) to assess the eye-activity correlates of motion sickness.

Relationship between spectra and road condition or motion sickness

As mentioned above, brain signals can be sensitive to any environmental change. Hence, the EEG signals acquired under various conditions (such as on a straight or curved road) are not confounded by motion-related activities. For example, when the experiment entered the winding-road riding section, the car began to sway left and right with the VR scene of the curved road, providing both visual and body sensation stimuli to the subjects. This baseline difference among EEG power spectra associated with the different road conditions must be considered when the MS-related EEG power changes are evaluated. Therefore, the EEG power spectral changes in three periods were initially examined: (1) baseline—the first 200 s of the baseline straight-road section, (2) low MS level—the first 200 s of the curved road section and (3) high MS level—the first 200 s after the highest sickness rating (Fig. 2A). The power spectra in these three time periods (baseline, low sickness and high sickness) were then averaged among subjects in each selected IC cluster.

A statistical analysis was also conducted to assess the significance of the spectral differences of the independent components under different motion-sickness levels and various road conditions. Since the true sample distribution of the component spectra was unknown and the sample size ($N = 19$ as 5 of 24 subjects were exclude due to extreme sickness levels) was small, a nonparametric statistical analysis, a paired-sample Wilcoxon signed-rank test, was employed to access the statistically significant spectral differences under different conditions. The level of significance was set to $p < 0.01$.

Time-frequency analysis

Time-frequency analysis was utilized to test the dynamics of the ICA power spectra throughout the experiment. The time series of the ICA power spectra were then correlated with the continuous sickness level to determine the MS-related spectral changes. The frequency responses of ICA activations were calculated using a 500-point moving window with 250 overlapping points. The 500-point epochs were further subdivided into several 125-point sub-windows with 25-point overlaps. The 125-point sub-windows were zero-padded to 512 points to calculate the power spectra using a 512-point fast Fourier transform (FFT), yielding an estimate of the power-spectrum density with a frequency resolution of 0.5 Hz. The power spectra of these sub-windows were then averaged to produce a power spectrum for each 2-s epoch. The power spectrum density (PSD) was then converted into decibel power. The temporal resolution of the resultant spectral time series was 1 s since the window step was 250 points and the EEG was sampled at 250 Hz.

MS-sorted EEG spectra

To examine the relationship between the severity of motion sickness and concurrent changes in the EEG spectrum, the EEG power spectra were first computed in the winding-road section, and the spectra were sorted by subjective MS level for each of the component. The sorted EEG spectrogram at each MS level was then averaged across the components within each IC cluster. A regression line was then plotted to determine the spectral change as functions of the MS level in each frequency band.

Causal relationship among MS-related EEG processes

Multiple components exhibited MS-related spectral changes. The causal relationship between these EEG processes is of interest. A cross-correlation analysis was performed on the power spectra of selected ICs for each individual. To be more specific, the spectral series at each frequency were temporally shifted from −200 to 200 s with a step size of 1 s and correlated with the time series of the subject's MS ratings. Finally, the results were averaged across components in each of the five IC clusters.

Results

ICA was separately applied to the EEG data from each subject, after bad channels and periods of data that contained disallowed or uncharacteristic artifacts were removed, to decompose the data into spatially fixed and temporally independent components. DIPFIT2 routines from EEGLAB were used to fit either one or sometimes two nearly bilaterally symmetric dipole source models to the component scalp topographies using a four-shell spherical head model (Oostendorp and Oostenveld, 2002). ICs were then clustered according to correlations among their dipole locations, time-frequency characteristics and overall power spectra.

Fig. 1 shows the equivalent dipole source locations and mean and individual scalp maps for five MS-related clusters from 19 sessions. These clusters had equivalent dipole sources in the left motor ($n = 13$), the parietal ($n = 11$), the right motor ($n = 11$), the occipital ($n = 14$) and the occipital midline ($n = 12$) areas. The two occipital IC clusters are separated based on the fact that the source locations of the occipital midline ICs are deeper than those of the occipital ICs.

Spectral changes under different conditions

Fig. 2 compares the mean component power spectra of the IC clusters under different motion-sickness levels and various road conditions. The EEG spectral difference associated with the different road conditions is observed by elucidated the baseline power spectra (green traces in Figs. 2B–F, from the very first 200 s of the baseline section) and the low MS level spectra (blue traces, from the first 200 s of the curve-road section). Evidently, the alpha powers of the right, left motor and the parietal components were suppressed from the straight-road driving to the winding-road driving as the car swayed from side to side. This finding suggests that these brain networks may be highly responsive to the movements of the platform and hence to somatic sensation. Further, the occipital midline IC cluster exhibited significant alpha power suppression (Fig. 2F).

Comparing the component power spectra under low MS level (blue traces in Fig. 2) and high MS level (red traces, 200-s period starting from the peak MS rating) revealed MS-related spectra changes. The red asterisks in Figs. 2B–F indicate the frequency bins where the component EEG power differed significantly between the maximum and minimum sickness levels under the same curve-road condition ($p < 0.01$, the paired-sample Wilcoxon signed-rank test). The alpha power of the occipital IC cluster (Fig. 2E) increased significantly with the MS level, whereas the occipital midline component cluster exhibited broadband spectral elevation at high MS. This result was perfectly in line with the results reported by Klimesch and colleagues (Klimesch, 1999; Klimesch et al., 1998).

Single-subject motion-sickness-related time-frequency responses

Time-frequency analysis was adopted to evaluate EEG correlates of fluctuations of MS level for the five selected IC clusters. Fig. 3 plots the time-frequency response of three ICs – occipital, parietal and right motor components – from 1 of the 19 subjects. The time-frequency responses of these three ICA components were evidently related to MS across time. Among these ICs, the correlation between the MS level and the changes in the alpha power in the occipital area (Fig. 3B) was the most pronounced. Furthermore, the changes in the alpha power in the parietal and the motor areas were also correlated with the MS levels (Figs. 3C and D).

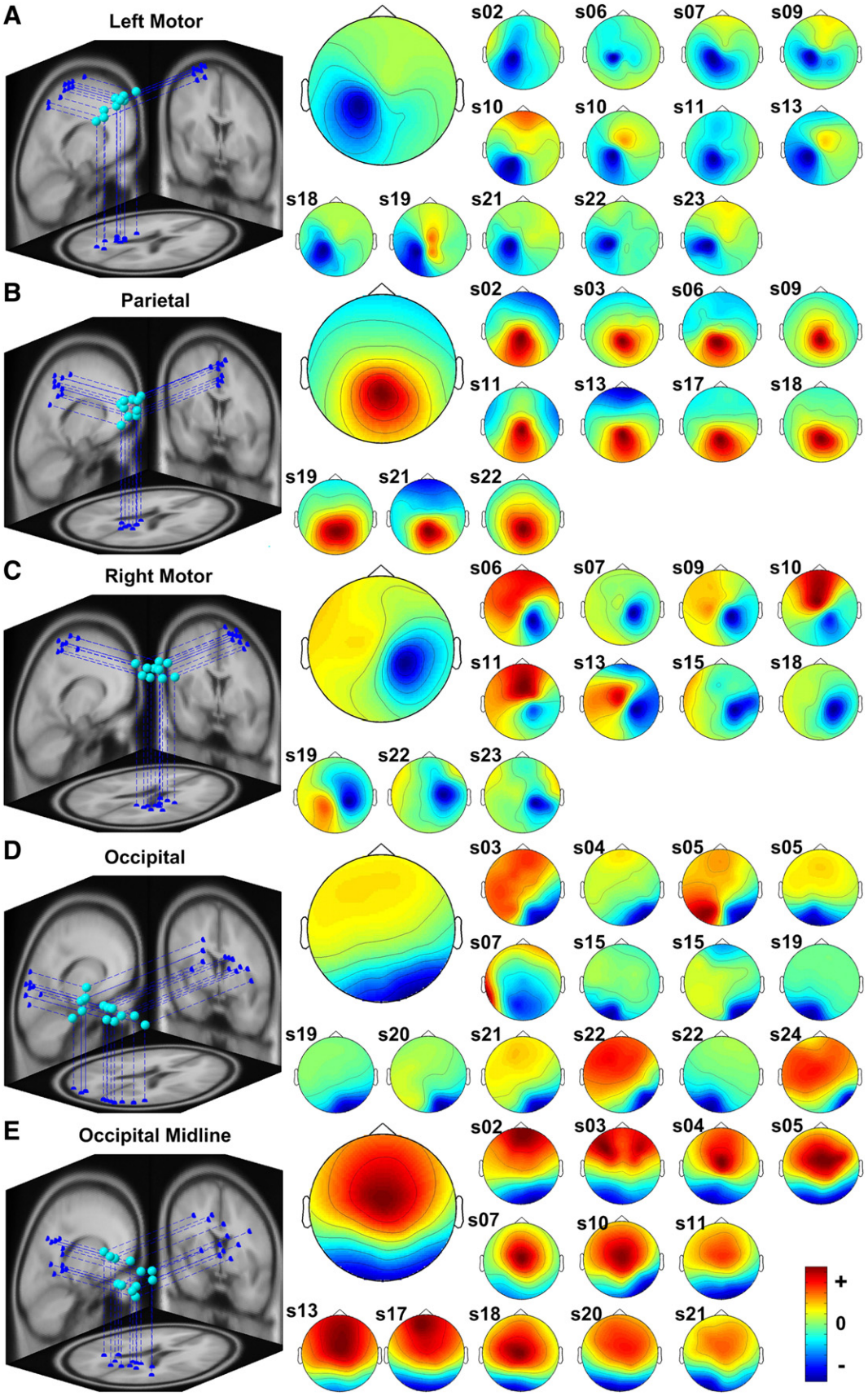

Fig. 1. Equivalent dipole source locations and mean and individual scalp maps for five IC clusters from 19 sessions. The 3D dipole source locations and their projections onto average brain images were given in the left panels. The single-subject scalp maps within each cluster and the averaged scalp maps were shown in the right panels. (A) left motor ($n = 13$), (B) parietal lobe ($n = 11$), (C) right motor ($n = 11$), (D) occipital ($n = 14$) and (E) occipital midline ($n = 12$).

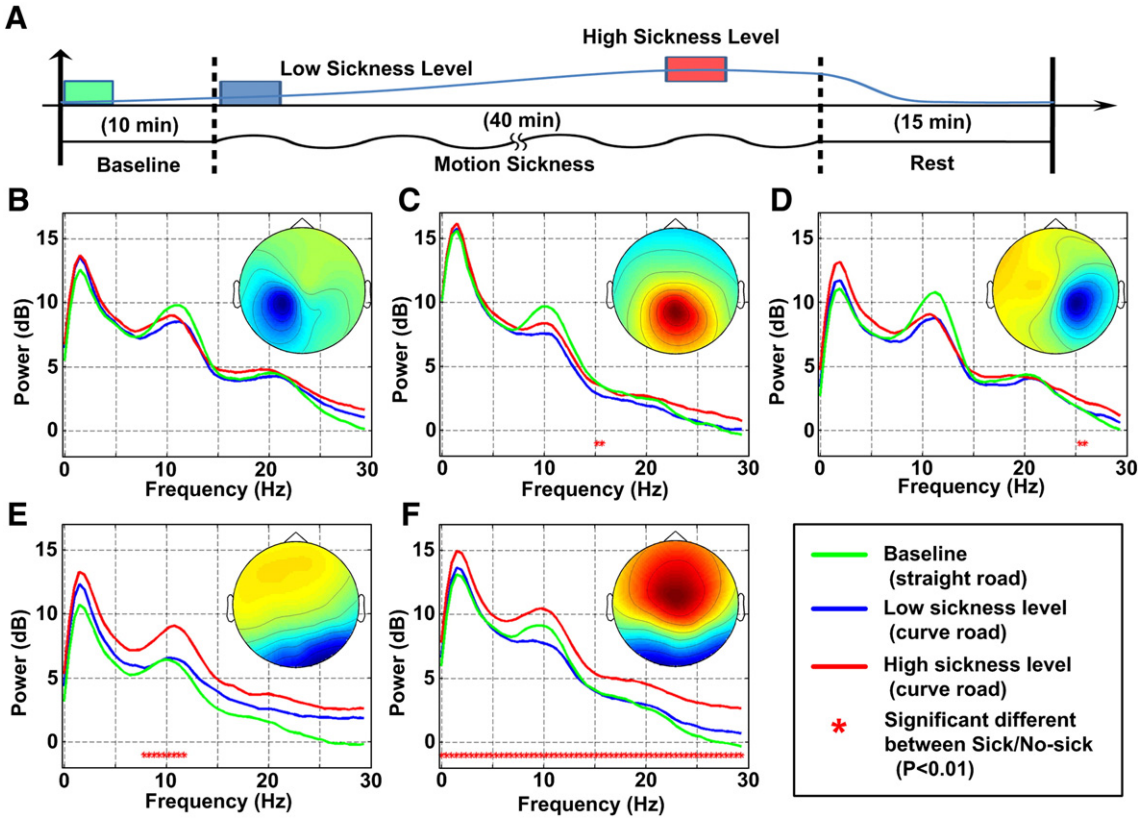

Fig. 2. Comparison of ICs' power spectra comparison under different motion-sickness levels and various road conditions. The averaged ICA power spectra of baseline (straight-road/no-sick) were shown as green lines, the power spectra of low sickness level (curve-road/no-sick) were shown in blue lines, and the power spectra of high sickness level (curve-road/sick) were shown in red lines. The red asterisks indicated the frequency bins where the component EEG power differed significantly between the maximum and minimum sickness levels under the same curve-road condition ($p < 0.01$, the paired-sample Wilcoxon signed-rank test).

Group MS-related spectral changes

To study the group EEG correlates of MS across subjects, the time-frequency responses of each subject were sorted first by level of motion sickness; the sorted time-frequency responses were then averaged across subjects. Fig. 4 plots the averaged group time-frequency responses that accompanied motion sickness for the five component clusters. The 3D plots reveal that the EEG power changes from low to high MS levels (1 to 5). The lower left 2D figures plot the net effects of MS on the spectra in different brain areas, obtained by subtracting the EEG power at low MS from the total EEG power in the 3D plots. Finally, a regression line was used to represent the linear relationship between the changes in EEG power and motion sickness. The gradient reveals the way in which MS level mediated the EEG power.

The left motor area (Fig. 4A) exhibited predominant spectral increases in all frequency bands as the MS level increased. The theta power increased by 3 dB, while the alpha and beta power increased by

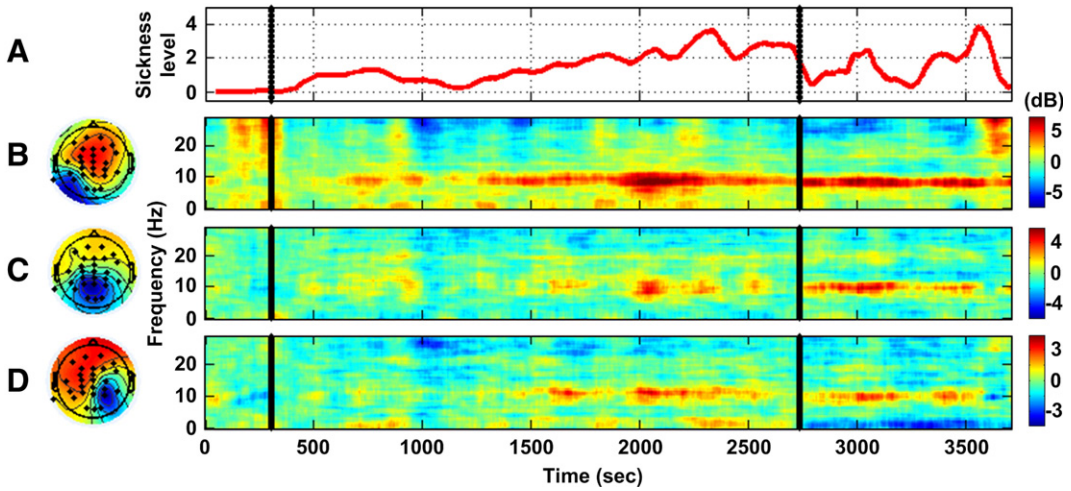

Fig. 3. Single-subject time-frequency results in the occipital, the parietal and the right motor components from one of the 19 subjects. (A) The recorded sickness level was shown in red. (B–D) Time-frequency responses of three ICA components co-varied with MS level at several frequency bands (see text).

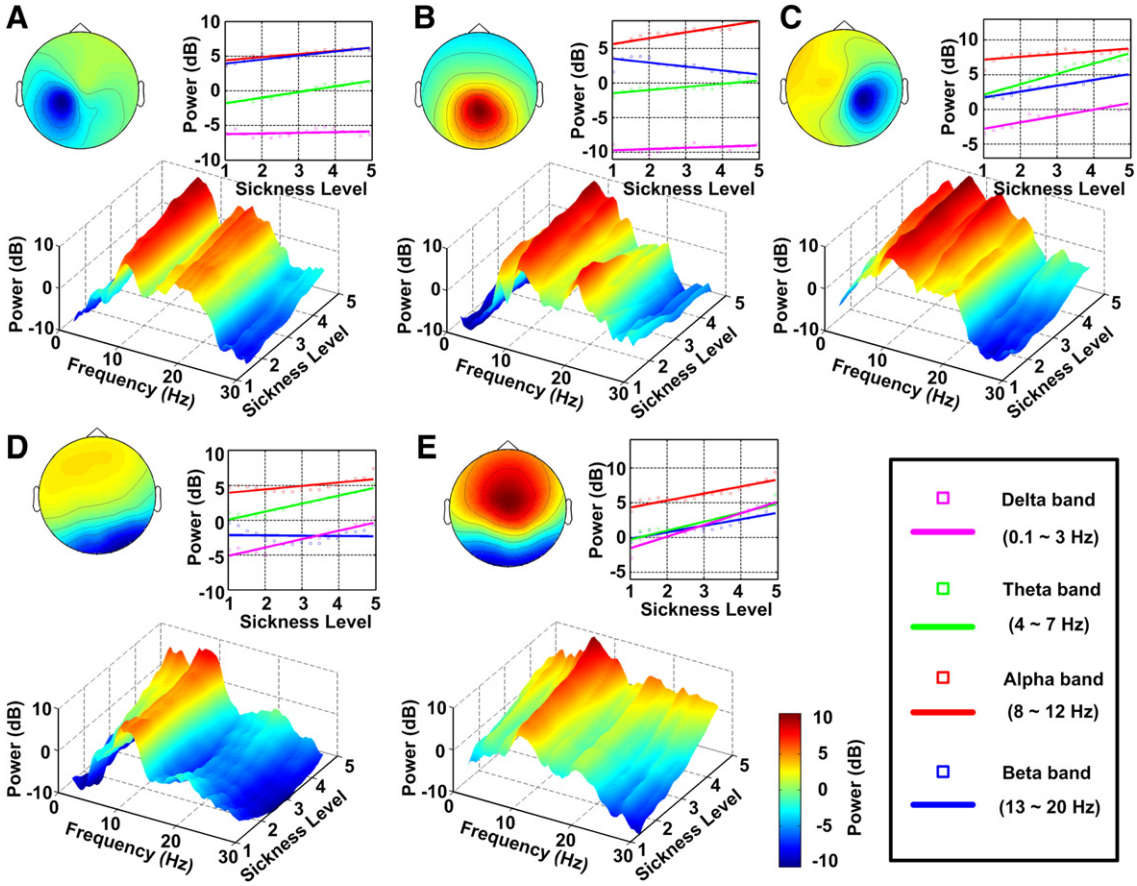

Fig. 4. The averaged group time-frequency responses during motion sickness for the five component clusters. The time-frequency responses of each IC were first sorted according to the sickness level. The sorted sickness-related time-frequency responses within each cluster were then averaged and plotted in the 3D plots. The 3D plots reveal that the EEG power changes from low to high MS levels (1 to 5). The lower left 2D figures plot the net effects of MS on the spectra in different brain areas, obtained by subtracting the EEG power at low MS from the total EEG power in the 3D plots. Shown are the linear trends of the EEG power changes in different frequency bands against the motion-sickness levels. A regression line was used to represent the linear relationship between the changes in EEG power and motion sickness. The gradient shown in lower right panels reveal the way in which MS level mediated the EEG power.

about 2 dB from the low MS (1) to high MS (5) state. The power spectra of the parietal components (Fig. 4B) increased in the delta, theta and alpha bands, while the beta-band power decreased by 2 dB as the MS level increased. The theta-band power increased by more than 5 dB in the right motor area (Fig. 4C) while the alpha-, delta- and beta-band power also increased slightly as the MS level increased. The

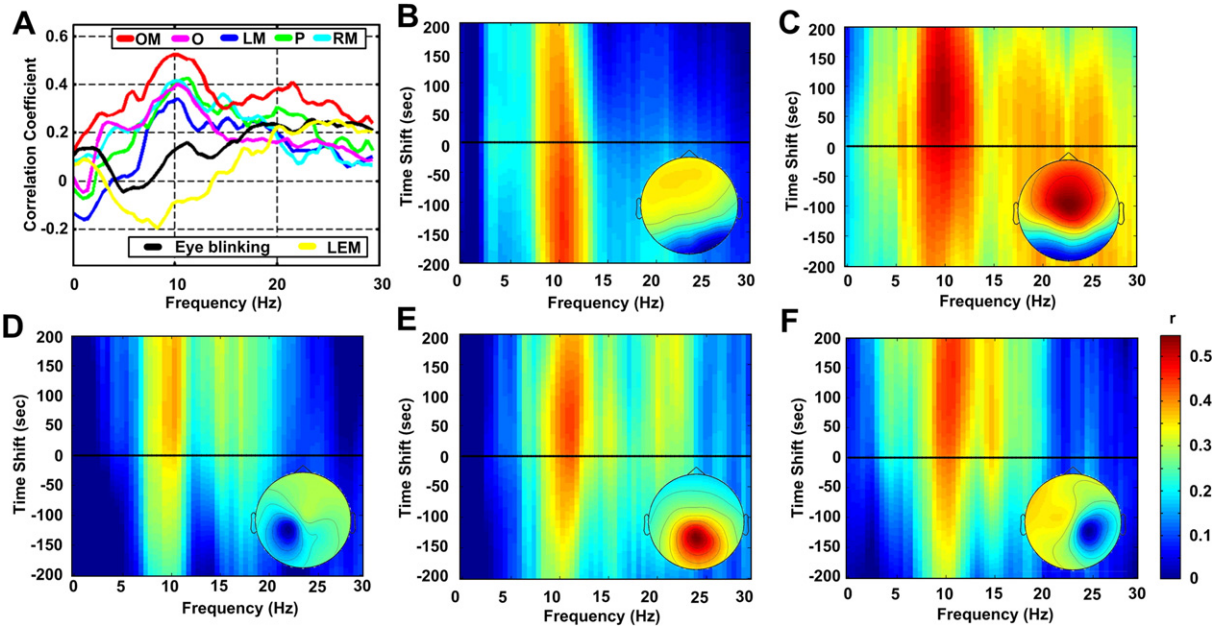

Fig. 5. The results of correlation and cross-correlation analysis between subjective sickness level and ICA power of the five brain areas. (A) The overall correlations between the component spectra and their corresponding MS levels of the five clusters. (B–F) The causal relationships between the MS-related EEG processes of the five independent clusters.

occipital components (Fig. 4D) also exhibited significant (more than 5 dB) spectral increases in the delta and theta bands. Increases in the broadband power spectra were observed in the occipital midline components, as presented in Fig. 4E.

Causal relationships between motion-sickness-related brain processes

Fig. 5A presents the overall correlations between the component spectra and their corresponding MS levels of the seven clusters. The correlation coefficients in the alpha band exceed those in other frequency bands in MS-related clusters. The maximum correlation coefficient in the alpha band is 0.5 in the occipital midline components, while the correlation coefficients are approximately 0.4 in other IC clusters. In addition, the maximum correlation coefficient between the time courses of the two eye-movement components and the MS level is 0.2.

The causal relationships between the MS-related EEG processes were computed and displayed in Figs. 5B–F. The highest correlation coefficients in the somatosensory areas (Figs. 5D and F) in the alpha band were obtained by shifting the sickness-level signals backward by approximately 100 s. The highest correlation coefficients of the parietal (Fig. 5E) and occipital midline (Fig. 5C) in the alpha band were obtained by shifting the behavior signals backward by about 80 and 60 s, respectively, whereas the highest correlation coefficients of the occipital (Fig. 5B) in the alpha band were obtained by shifting the sickness-level signals forward by about 120 s.

The results suggest that the independent EEG components can be used to predict the onset of motion sickness. Some of them preceded the subjects' sickness ratings, such as the alpha power in the somatosensory areas, which fact might reflect the suppression of vestibular inputs to eliminate the conflict with subjects' visual perception. Then, at approximately 60 s before subjects reported their motion sickness, the occipital midline area began to exhibit the MS-related alpha power increases. Moreover, this independent component exhibits the strongest correlation with the motion-sickness rating. Consequently, this IC cluster may be a potential index to predict the onset of motion sickness.

Discussion

This study elucidates EEG correlates of motion sickness in a realistic VR- and motion-platform-based driving simulator. The recorded EEG data of each subject were first decomposed using ICA to isolate the spatially fixed and temporally independent EEG processes from the noise and artifacts. The time courses of spectral changes of these independent EEG components were then correlated with the subject's motion-sickness ratings that were simultaneously recorded during the experiment.

Modalities to induce motion sickness

The sensory conflict theory proposes that motion sickness may be caused by the receipt of incongruent information from the multi-modal somatosensory system, including visual information and most importantly, vestibular sensations. Thus, most studies in the field have introduced conflicting multi-modal somatosensory information to induce motion-sickness symptoms. Some have employed the rotary chair (Wood et al., 1991, 1994) or the parallel swing (Wu, 1992), which create bodily movement without corresponding visual cues, and further generated incongruent somatosensory inputs. Others have adopted visual stimuli with no vestibular input, such as by using cross-coupled angular stimulation (Chelen et al., 1993), the optokinetic drum (Hu et al., 1999) or other forms of stimulation (Lo and So, 2001; Kim et al., 2005; Min et al., 2004), to induce motion-sickness symptoms. However, since motion-sickness involves the multi-modal somatosensory system, the incorporation of both visual and vestibular stimuli into the motion-sickness studies is more realistic. Combining a VR scene with a dynamic motion platform provides a more complete environment in which to investigate the effect of the motion sickness on cognitive states, as well as the underlying neurophysiology. In this study, this combined modality is used to induce near-real-world motion sickness.

MS-related spectral changes

Figs. 4A–C reveal that the alpha power increases with the MS level, especially in the parietal lobe. This result is consistent with the results of a gravitational experiment that was conducted by Cheron et al. (2006), who determined that 10-Hz oscillations in the parieto-occipital and sensorimotor areas increased as gravity was removed. They also suggested that since the parietal lobe is situated at a transition between the somatosensory and the motor cortex, it may therefore be involved in the integration of spatial representation, which requires body sensation information from vestibular inputs.

In the right and left motor areas, the increases in the theta-band power are greater than those in the delta, alpha and beta bands (Figs. 4A and C). Such theta power increases have also been recorded in numerous studies of motion-induced motion sickness. However, the brain areas that have been associated with the theta power increases are not completely consistent. Wu (1992) reported theta power increases in the frontal and central areas in a parallel swing study. Significant MS-related theta power increases have been induced in the frontal areas using a rotating chair (Wood et al., 1991, 1994). However, Chelen et al. (1993) reported theta power increases in the temporo-frontal in a cross-coupled angular stimulation experiment.

The theta power increases can be referred to sensorimotor integration, which were demonstrated in a way-finding VR experiment by Caplan et al. (2003). They found theta oscillations in the peri-Rolandic regions and the temporal lobes were related to (1) movement (both virtual and real), (2) updating the motor plan according to the information collected from a multi-modal somatosensory system and (3) coordinating with the internal map during navigation. However, in the experiment in this study, the subjects were instructed to report their motion-sickness levels using a joystick only. The subjects had to report no further navigation information (such as number and degree of turns and related information). Although the real turns may unavoidably influence navigation function of the subjects, their effect should be relatively limited. Moreover, the possibility of motion-induced theta power changes was eliminated by removing the EEG power changes that were related to the baseline under the two experimental conditions—baseline straight-road and baseline curve-road conditions. Consequently, the theta power increases found in the two motor areas were caused mainly by the integration of the multi-modal somatosensory information, which may be essential to the motor planning of bodily movement in response to the motion of the platform during cruising on the curved road. Additionally, Caplan et al. (2003) claimed that the effect of the theta power increase was asymmetric across the left and right hemispheres. The power increase is more pronounced in the right hemisphere than in the left. The results herein were consistent with their findings (Figs. 2B and D). Bland and Oddie (2001) also developed the sensorimotor integration hypothesis, according to which theta oscillations act to coordinate activity in various brain regions to update motor plans in response to somatosensory inputs. Jensen (2001) demonstrated that theta oscillations act as carrier waves for information transfer between any pair of regions via synchronized oscillations at the same frequency.

In the occipital midline component cluster (Fig. 4E), component spectra monotonically increased with the MS level in all frequency bands (delta, theta, alpha and beta). Such a broadband power increase

may indicate that motion sickness can strengthen the underlying brain processes, perhaps because of the difficulty of the task during motion sickness. This result may also indirectly demonstrate conflicts within multi-modal somatosensory systems as they sense the environment around the subject, causing the related brain circuits to work harder than at the baseline (no motion-sick condition). According to the results of the correlation analysis (Fig. 5A), in the occipital midline cluster, the EEG power responses in the occipital midline were more highly correlated to subjective sickness levels than in other brain areas, suggesting that activations in the occipital midline may be useful in determining the stages of motion sickness.

Although determinations by various studies of the brain regions that are involved in motion-sickness remain inconclusive, many studies have presented delta power increases. For example, an increase in delta-band power was observed at C3 and C4 in an optokinetic rotating drum experiment (Hu et al., 1999) and in the frontal and temporal areas in an object-finding VR experiment (Kim et al., 2005). A delta power increase at Fz and Cz was also found in a VR-based car-driving experiment conducted by Min et al. (2004). Furthermore, a delta power increase has also been reported in a motion-induced motion-sickness study using cross-coupled angular stimulation (Chelen et al., 1993). In that study, the delta power increase was detected over the occipital, the occipital midline and the right motor IC clusters (Figs. 4C–E), mainly during the curved-road section (Fig. 3). This change in EEG power may be treated as a stress component caused by the motion sickness or violent movement of the motion platform, as suggested by Chen et al. (1989).

The resultant spectral changes might be due to a confounding effect of moving a joystick and motion sickness. However, the joystick movements were very sparse as the subjects did not need to move the joystick unless they felt the level of motion sickness has been changed. Previous studies (Huang et al., 2007; Huang et al., 2008) showed that the spectral changes following finger/hand movements in the sustained attention tasks were usually transient (a quick spectral suppression followed by an equal-amplitude rebound within 2–4 s). Furthermore, these spectral perturbations would be the same regardless if the subject reported an increase or a decrease in the sickness level. Thus, the joystick movements would not have biased the spectral correlates toward to a spectral increase or decrease systematically when the correlation between the time course of component spectra and the subjective sickness level was calculated in a much longer (smoothed) time scale.

Time delay

Cross-correlation analysis between the subjective sickness level and the power spectra of the independent EEG components facilitates an investigation of the underlying neurophysiology of motion sickness in the human brain. Our analysis results revealed a strong positive cross-correlation of the subjective sickness level with spectra at 10 and 15 Hz of the two motor IC clusters, leading the peak of the subjective MS rating by 100 s, possibly indicating the difficulty of integrating multi-modal somatosensory information into the motor-planning process or compensation of the movement of the motion platform, resulted in the suppression of the bilateral motor control-related brain circuits. However, a strong cross-correlation existed with the alpha and beta spectra in the parietal and the occipital midline areas, leading the MS rating peaks by 80 and 60 s, respectively (Figs. 5C and E). This finding may correspond to the extra loading associated with the integration of multi-modal somatosensory information during motion sickness and the "perception" that motion sickness is approaching its most severe. In the occipital IC cluster, the alpha power increase is more pronounced than the spectral increases in other frequency bands (Fig. 2E). In the literature, alpha activity has been regarded as the resting rhythm and has been identified as cortical idling in a way-finding experiment by Caplan et al. (2003). The changes in alpha power were much (~120 s) later than those of the subjective motion-sickness ratings, suggesting that this rhythmic activity may be related to relaxation after the long stress that is caused by the motion-sickness section.

Conclusions

By combining independent component analysis, time-frequency analysis and cross-correlation analysis, this work evaluates changes in the EEG power spectrum that accompanies the fluctuations in the level of motion sickness in a realistic driving task. ICA separates the multi-channel EEG signals into independent brain processes, each of which represents electrical neurophysiological activities from a tight cluster of neurons. Components with similar scalp tomography, dipole location and baseline power spectrum from multiple subjects were grouped into component clusters. The sorting and correlation of power spectra with subjective MS levels reveal a monotonic relationship between minute-scale changes in MS and the EEG spectra of distinct component clusters (brain processes) in different frequency bands. In summary, this (1) utilized both visual and vestibular stimuli to induce realistic motion sickness, (2) proposed a continuous rating mechanism using which subjects can report their MS level without interrupting the experiment and (3) evaluated reproducible spectral changes in multiple brain areas that accompany fluctuations in the severity of motion sickness.

Acknowledgments

The authors want to thank Li-Shuo Hsiao and Teng-Yi Huang for developing and preparing the VR-based motion sickness experiments. This work was in part supported by the Aiming for the Top University Plan of National Chiao-Tung University, the Ministry of Education, Taiwan, under Contract 98W806, and in part supported by the National Science Council, Taiwan, under Contracts NSC 97-2627-E-009-001 and NSC 97-2221-E-009. Finally, the authors would like to thank the reviewers for their constructive comments that help improve this article.

References

Bell, A.J., Sejnowski, T.J., 1995. An information-maximization approach to blind separation and blind deconvolution. Neural Comput. 7 (6), 1129–1159.
Bland, B.H., Oddie, S.D., 2001. Theta band oscillation and synchrony in the hippocampal formation and associated structures: the case for its role in sensorimotor integration. Behav. Brain Res. 127 (1-2), 119–136.
Caplan, J.B., Madsen, J.R., Schulze-Bonhage, A., Aschenbrenner-Scheibe, R., Newman, E.L., Kahana, M.J., 2003. Human θ oscillations related to sensorimotor integration and spatial learning. J. Neurosci. 23 (11), 4726–4736.
Chelen, W.E., Kabrisky, M., Rogers, S.K., 1993. Spectral analysis of the electroencephalographic response to motion-sickness. Aviat. Space Environ. Med. 64 (1), 24–29.
Chen, A.C., Dworkin, S.F., Haug, J., Gehrig, J., 1989. Topographic brain measures of human pain and pain responsivity. Pain 37 (2), 129–141.
Ch eron, G., Leroy, A., De Saedeleer, C., Bengoetxea, A., Lipshits, M., Cebolla, A., Servais, L., Dan, B., Berthoz, A., McIntyre, J., 2006. Effect of gravity on human spontaneous 10-Hz electroencephalographic oscillations during the arrest reaction. Brain Res. 1121, 104–116.
Cheung, B., Vaitkus, P., 1998. Perspectives of electrogastrography and motion-sickness. Brain Res. Bull. 47 (5), 421–431.
Delorme, A., Makeig, S., 2004. EEGLAB: an open source toolbox for analysis of single-trial EG dynamics including independent component analysis. J. Neurosci. Methods 134, 9–21.
Holmes, S.R., Griffin, M.J., 2001. Correlation between heart rate and the severity of motion-sickness caused by optokinetic stimulation. J. Psychophysiol. 15 (1), 35–42.
Hu, S., Grant, W.F., Stern, R.M., Koch, K.L., 1991. Motion-sickness severity and physiological correlates during repeated exposures to a rotating optokinetic drum. Aviat. Space Environ. Med. 62 (4), 308–314.
Hu, S., McChesney, K.A., Player, K.A., Bahl, A.M., Buchanan, J.B., Scozzafava, J.E., 1999. Systematic investigation of physiological correlates of motion-sickness induced by viewing an optokinetic rotating drum. Aviat. Space Environ. Med. 70 (8), 759–765.
Huang, R.S., Jung, T.P., Makeig, S., 2007. Event-related brain dynamics in continuous sustained-attention tasks. In: Schmorrow, D.D., Reeves, L.M. (Eds.), Augmented Cognition, HCII 2007, LNAI 4565, pp. 65–74.

Huang, R.S., Jung, T.P., Delorme, A., Makeig, S., 2008. Tonic and phasic electroencephalographic dynamics during continuous compensatory tracking. NeuroImage 39, 1896–1909.
Jensen, O., 2001. Information transfer between rhythmically coupled networks: reading the hippocampal phase code. Neural Comput. 13, 2743–2761.
Jung, T-P, Makeig, S., Humphries, C., Lee, T-W., McKeown, M.J., Iragui, V., Sejnowski, T.J., 2000. Removing electroencephalographic artifacts by blind source separation. Psychophysiology 37, 163–178.
Kennedy, R.S., Lane, N.E., Berbaum, K.S., Lilienthal, M.G., 1993. Simulator sickness questionnaire: an enhanced method for quantifying simulator sickness. Int. J. Aviat. Psychol. 3 (3), 203–220.
Kim, Y.Y., Kim, H.J., Kim, E.N., Ko, H.D., Kim, H.T., 2005. Characteristic changes in the physiological components of cybersickness. Psychophysiology 42, 616–625.
Klimesch, W., 1999. EEG alpha and theta oscillations reflect cognitive and memory performance: a review and analysis. Brain Res. Brain Res. Rev. 29, 169–195.
Klimesch, W., Doppelmayr, M., Russegger, H., Pachinger, T., Schwaiger, J., 1998. Induced alpha band power changes in the human EEG and attention. Neurosci. Lett. 244, 73–76.
Lo, W.T., So, R.H.Y., 2001. Cybersickness in the presence of scene rotational movements along different axes. Appl. Ergon. 32, 1–14.
Makeig, S., Jung, T.P., Bell, A.J., Ghahremani, D., Sejnowski, T.J., 1997. Blind separation of auditory event-related brain responses into independent components. Proc. Natl. Acad. Sci. U. S. A. 94, 10979–10984.
Min, B.C., Chung, S.C., Min, Y.K., Sakamoto, K., 2004. Psychophysiological evaluation of simulator sickness evoked by a graphic simulator. Appl. Ergon. 35, 549–556.
Oostendorp, T.F., Oostenveld, R., 2002. Validating the boundary element method for forward and inverse EEG computations in the presence of a hole in the skull. Hum. Brain Mapp. 17, 179–192.
Wood, M.J., Struve, F.A., Straumanis, J.J., Stewart, J.J., Wood, C.D., 1991. The effect of motion-sickness on brain waves (EEG). Aviat. Space Environ. Med. 62, 461.
Wood, C.D., Stewart, J.J., Wood, M.J., Struve, F.A., Straumanis, J.J., Mims, M.E., Patrick, G.Y., 1994. Habituation and motion-sickness. J. Clin. Pharmacol. 34, 628–634.
Wu, J.P., 1992. EEG changes in man during motion-sickness induced by parallel swing. Space Med. Med. Eng. 5 (3), 200–205.